From polyethyleneimine hydrogels to Pickering-like smart "On/Off" emulgels switched by pH and temperature

Gregory Douyere, Loïc Leclercq, Véronique Rataj

From Polyethyleneimine Hydrogels to Pickering-like Smart "On/Off" Emulgels Switched by pH and Temperature

Grégory Douyère, Loïc Leclercq*, Véronique Nardello-Rataj*

Univ. Lille, CNRS, Centrale Lille, Univ. Artois, UMR 8181 - UCCS - Unité de Catalyse et Chimie du Solide, F-59000 Lille, France. loic.leclercq@univ-lille.fr ; veronique.rataj-nardello@univ-lille.fr. tel : +33(0)3.20.33.63.69

Abstract.

Hypothesis: According to the so-called colloidal tectonic concept, we assumed that a single self-complementary polymer-based tecton could be used to design self-assembled emulsions. The polymer must be of high-molecular weight with balanced bipolar properties generating those of rigidity and flexibility. Linear polyethyleneimine (LPEI, 25k Da) was used because it acts as a buffer by continuous protonation/deprotonation of the amine groups.

Experiments: The relationships between the physicochemical properties of LPEI (protonation, charge, size, aggregation and gelation) and emulsions (type, droplet size, rheological behavior and stability) were investigated to highlight the self-assembly and stabilization mechanisms during the construction events as well as the inherent properties of emulsions (responsiveness to external stimuli).

Findings: In aqueous solution, after a first heat and cool cycle, the adequate and spontaneous self-assembly of hydrophobic and hydrophilic sections leads to hydrogels by the formation of a 3D network where the crystallized hydrophobic domains act as knots. In the presence of various oils, the hydrogels provide long-term stable Pickering emulgels. The as-prepared emulsions are highly controllable due to their self-assembled nature (up to 10 consecutive runs). Consequently, this new approach provides a facile route to construct self-assembled, reversible and dynamics Pickering-like emulsions by simplifying the colloidal tectonics concept.

Keywords: Polyethyleneimine hydrogels, Colloidal tectonics, Pickering emulgels, Multi-responsive systems, Temperature, pH

1. Introduction

Since the last two decades, Pickering emulsions have aroused considerable interest in diverse areas including industry, agriculture, medicine and cosmetics [1-6]. This broad interest is mainly linked to their long-term stability due to the absorbed particles on the water/oil interfaces which prevent coalescence [1,4]. Unfortunately, even though Pickering emulsions are an elegant way to avoid environmentally unfriendly molecular surfactants, their human health risks depend on the nature of the stabilizer [7]. Indeed, inorganic-based nanoparticles (NPs) are widely used to stabilize Pickering emulsions but their potential hazardous effects on human health are a matter of increasing interest and concern [8,9]. For instance, the European Commission on Public Health cautioned that NPs might have the ability to cross cell membranes into a living system [10]. Thus, silica NPs, depending on their dimensions, are suspected of being able to penetrate into and through the skin with potential toxicity due to their accumulation and persistence in living systems [11].

In this context, a smart alternative is to exploit the colloidal tectonics concept based on the engineering of Pickering emulsions from the self-assembly of molecular building blocks (tectons) without any synthetic steps [12]. For instance, aqueous solutions of α-cyclodextrin and polyethylene glycol (α-CD and PEG), on cooling conditions, lead to the following self-recognition events: (*i*) host-guest interactions between the two tectons lead to α-CD/PEG polypseudorotaxanes, (*ii*) H-bonds between neighboring α-CDs initiating a crystallization of the CD rich domains, and (*iii*) hydrogelation due to crystallites acting as knots alongside the not-included PEG chains [12]. In the presence of oil, hydrogels provide Pickering emulsions which can be advantageously used for drug delivery since their dissociation into molecular tectons limits harmful side effects and/or accumulation in living systems, unlike those based on conventional NPs [13]. In the light of this system and the few others known, it is admitted that the colloidal tectonics requires at least two self-complementary tectons, one of which is "hydrophobic" and the other "hydrophilic" (with at least a rigid structure for one of them) [12]. These requirements do not seem absolutely necessary. Indeed, high-molecular weight polymers with appropriate hydrophilic and hydrophobic "segments" could

allow the hydrogelation by aggregation and crystallization of hydrophobic sections *via* a similar mechanism of α-CD/PEG system [13,14]. Nevertheless, the crystallites must also be stable in organic solvents to serve as Pickering emulsifiers, *i.e.* crystal packing energy must be higher than molecular solvation [12]. In addition, for practical applications, stimulus-responsive systems are required to counterbalance long-term stability with appropriate triggers (*e.g.* pH, temperature) leading to rapid phase separation [15]. Consequently, finding suitable polymers for this remains a challenge.

Linear and branched polyethyleneimines (LPEIs and BPEIs, respectively) are produced on an industrial scale, available in a broad range of molecular weights, and widely used in the biological field, *e.g.* drug or gene delivery, transfection, permeabilization of bacteria [16]. All BPEIs are water-soluble while LPEIs are insoluble in cold water and organic solvents (*e.g.* alkanes, aromatics) but soluble in hot water and/or at low pH [17]. Consequently, high-molecular weight LPEIs seem to be ideal to provide an inexpensive responsive-tecton since the solubility as well as the hydrophilic/hydrophobic balance can be easily adjusted by protonation and temperature change. To our knowledge, PEIs have never been used alone to produce Pickering emulsions but only to adjust the wettability of inorganic, organic or bio-based NPs (clay, silica or cellulose) by physical or chemical surface functionalization leading to hybrid systems [18-23]. Unfortunately, these hybrid NPs are not straightforward as they potentially require harmful synthetic steps. In addition, toxicity induced by skin binding and penetration is not resolved for PEI-modified inorganic NPs.

Here, the colloidal tectonics concept is applied to LPEI, as the sole tecton, to easily build up a switchable gelled Pickering emulsions. We used the LPEI (25k Da) as a model tecton because of its commercial availability and its potential application to permeabilize bacterial cells. In this study, we particularly focus on the concept description and proof of the concept to demonstrate the user-friendly access and versatility of these tunable colloidal systems. Indeed, the as-prepared emulgels show high stability but can be destabilized by pH and temperature changes leading to "on-off" switching service due to a continuous transition of properties between the tecton and the emulsion.

2. Materials and methods

2.1. Materials and general information

LPEI (25k Da), paraffin oil (> 99 %), HCl (34 %) was purchased from Alfa Aesar (USA), Cooper (France) and Verbiese (France), respectively. All the other chemicals of analytical grade were obtained from Merck KGaA (Germany) and were used as received without further purification. Ultrapure, double distilled water, passed through a reverse osmosis system and further treated with a Barnstead water purification system (18.2 MΩ.cm at 25 °C, Thermo Scientific, USA) was used for all experiments. The temperatures were stabilized using temperature-controlled water bath with a precision of ±0.02 °C (Huber Ministat 125 Cryothermostat, Germany). To ensure repeatability, all measurements were performed three times. Sonications were performed using an UP200St equipped with a sonotrode S26d7 (Hielscher Ultrasonic, Germany) in a thermo-regulated bath at 25 °C to avoid overheating due to ultrasound. Centrifugations were performed with a Sigma 2-16PK (Sigma, Germany). Data fitting was performed with OriginPro 8® (OriginLab, USA). The contact angles were measured according to the spreading method by depositing solvent (4 µL) on compressed particles (1,800 bars, 1 min) using DSA 100 analyzer (Krüss GmbH, Germany).

2.2. Characterization of the LPEI aqueous dispersions

In this section, the temperature is always kept at 25 °C using a temperature-controlled water bath to avoid the hydrogel formation (see section 2.3). In more detail, aqueous solutions or dispersions of LPEI (0.1 wt.%), prepared at various initial pH, from 1 to 13 using stock HCl or NaOH solutions (0.5 M), were homogenized or dispersed with an ultrasonic probe for 2 min with an amplitude of 30% and a pulse of 50%. The system was left equilibrating at 25 °C overnight. The electrical conductivity and pH were measured with a pH330i (WTW, Germany) and CDM210 (Radiometer Analytical, France) whereas the ζ-potential and size were made using a Zetasizer Nano ZS ZEN 3600 (Malvern Instruments, UK). The ζ-potentials were collected from the velocities of LPEI molecules or aggregates submitted to an external electric field by laser interferometric using the Smoluchowski

approximation. The size of LPEI molecules or aggregates were collected by dynamic light scattering at 173° using time-correlation functions. Data were analyzed by cumulative analysis to obtain an average diffusion coefficient used to calculate a hydrodynamic radius using the Stokes-Einstein equation. The physical stability of dispersions was evaluated using a Turbiscan Lab Expert (Formulaction, France) at 25 °C. The stability index (SI), corresponding to the sum of variations of backscattering (ΔBS) at a given time, was calculated as implemented in the TurbiSoft-Lab software.

2.3. Preparation and characterization of LPEI-based hydrogels

LPEI (0.1 to 5 wt.%) was dispersed in water at 25 °C and heated at 70 °C (1 °C/min, 300 rpm). The obtained LPEI hydrogels in the sol phase were then kept for 15 min at 70 °C before cooled at room temperature for 6 h without stirring to give the hydrogel in the gel phase. The thermo-responsive behavior of hydrogels was analyzed by successive heat and cool cycles (1 °C/min, 300 rpm). The solubilisation and gelation frontiers were evaluated through visual and microscopic observations. These last were obtained using a light digital microscope (VHX-900F equipped with a VH-Z100UR/W/T lens, Keyence, France). Rheological properties were evaluated using a Kinexus rheometer (Malvern Instrument, UK) equipped with a parallel-plate geometry (20-mm diameter and 1-mm gap) and a Peltier temperature control device with an accuracy of 0.01 °C. Stress-controlled measurements were performed imposing a logarithmic stress ramp increase followed by a reverse stress decrease, from 0 to 500 Pa. Temperature-controlled measurements from 20 to 70 °C (1 °C/min) were also conducted at a fixed shear rate (100 s^{-1}).

2.4. Preparation and characterization of LPEI hydrogels-based Pickering emulsions

Emulsions were prepared from the previous hydrogels (see the section 2.3) by adding oil. However, in the final emulsions, the water/oil ratios were fixed at 1:1 w/w. For instance, 0.5 wt.% LPEI emulsion was prepared from a hydrogel composed of 0.5 wt.% of LPEI and 49.75 wt.% of water. Then the resulting hydrogel was supplemented with 49.75 wt.% of oil before emulsification in a 5

mL container using an Ultraturrax (T10 basic, IKA, Germany) equipped with the S10N-8G dispersing element (11,500 rpm, 60 s, 25 °C). The emulsion type was determined by conductivity measurement. Optical microphotographs were obtained as previously described (see section 2.3). In more detail, the droplets size distribution was obtained by fitting at least 200 individual droplet diameters obtained using ImageJ (NIH, USA) with a log-normal function (OriginPro 8®, OriginLab, USA). The stability of emulsions was evaluated using the variation of ΔBS profiles over 2 days at 25 °C (see section 2.2). Rheological properties of emulsions were conducted as previously described in the section 2.3. The dynamic oscillatory shear tests were performed from 0.1 to 10 Hz with a fixed strain of 0.1 % to ensure that all measurements were carried out in the linear viscoelastic region leading to the storage (G') and loss moduli (G").

2.5. Reversibility of LPEI hydrogels-based emulsions

The reversibility of the emulsions (containing 2 wt.% of LPEI and hydrogel-to-oil ratio equal to 1) was evaluated as a function of temperature and pH. For instance, thermo-reversibility was achieved after successive heat and cool cycles. Indeed, a total phase separation was obtained at 75 °C whereas the re-emulsification was easily achieved after cooling to 25 °C (11,500 rpm, 60 s). Similarly, pH-reversibility was succeeded by cycling pH between 8 and 5. On stimulating at acidic pH (by addition of aqueous HCl until to reach pH 5), the system started to demulsify. The complete phase separation was achieved using $4,024 \times g$ as centrifugation speed. But when the system was re-treated at pH 8 (by addition of aqueous NaOH), the hydrogel was reformed and re-emulsified (11,500 rpm, 60 s, 25 °C).

3. Results and discussion

3.1. Effect of pH on LPEI species in aqueous solution.

LPEI is commercialized in free base form, the LPEI is unprotonated and hydrophobic because of its ethylene-rich and uncharged backbone. In such conditions, the polymer aggregates thanks to hydrophobic interactions and becomes insoluble in pure water at 25 °C [24]. This strong tendency of

LPEI to aggregate is typical of perfectly linear, unsubstituted and flexible polymers. However, it is noteworthy that the aggregation is also enhanced by the formation of H-bonds [24]. Indeed, hydrophobic interactions is complemented by the H-bonds between the LPEI chains themselves (N−H⋯N) and by the hydration layers *via* the formation of O−H⋯N and N−H⋯O bonds preventing the aggregated polymers from entering in contact with each other and maintaining the integrity of crystalline or pseudo-crystalline aggregates [24]. According to their history, these polyamines can be hydrated leading to a complex system of H-bonds. In our case, we can assume that the dispersion of LPEI in aqueous solution results in more of less hydrated structures in which the direct bonds between the amino groups are at least partially replaced by bonds with water molecules [25]. Indeed, the water molecules can link the parallel segments of the LPEI chains *via* the O−H⋯N and N−H⋯O bonds. Additionally, H−O⋯H bonds can connects water molecules between the chains (see Figure 1). The X-ray diffraction (XRD) patterns of LPEI powders suggest ordered crystals due to the presence of three intense bands at $2\theta = 17, 23$ and $25°$ characteristic of pure crystalline hydrated LPEI structures that remain completely insoluble at room temperature [25]. The hydrate nature is confirmed by the dehydration between 125 and 140 °C and the formation of solution at high temperatures. Indeed, in hot water, the N−H⋯N bonds between the amino groups are dissociated and are replaced by H-bonds between the LPEI chains and the surrounding water molecules. The gelation during cooling may occur due to the competition between the H-bonds leading to solvated and aggregated sections (see below). Another method to achieve complete solubilisation in water environment at room temperature is to protonate the amino groups of LPEI by adding HCl. As all the charges are positioned directly on the backbone of the chain, the maximum distance between the two neighbor charges is very small, resulting in an extended conformation due to electrostatic repulsions [26]. This also takes place between the LPEI chains, preventing the hydrophobic attractive interaction and the H-bonds between the LPEI chains. However, the backbone extension of LPEI depends on the balance between inter- and intra-chain interactions regulated by pH (Figure 1). Indeed, at low pH, the high electrostatic repulsions, between the positively charged amine groups, favor an extended backbone of the LPEI

(intra-chain repulsions) and avoid the inter-chain hydrophobic attractions (❶ is the dominant species, see Figure 1) [26]. Therefore, the highly protonated LPEI is water-soluble. When the homogeneous LPEI solution is gradually deprotonated, longer sequences of neutral LPEI appear. Consequently, the LPEI firstly folds in such a way that these neutral sequences are buried into the interior part of the structure, minimizing their contact with water (❷ is the dominant species) [26]. Secondly, the more the electrostatic repulsions are screened, the more the LPEI behaves like neutral hydrophobic polymer and some LPEI chains tend to aggregate (❸ is the dominant species) [26]. For these last species, the system remains dynamic: the enthalpy of aggregation provides the energy to rearrange the protons distribution on the LPEI chains leading to an increase of protonated amine groups on the surface of the LPEI aggregates, minimizing their desolvation. For very high pH, the system is totally collapsed (total precipitation, ❹ is the dominant species) [26].
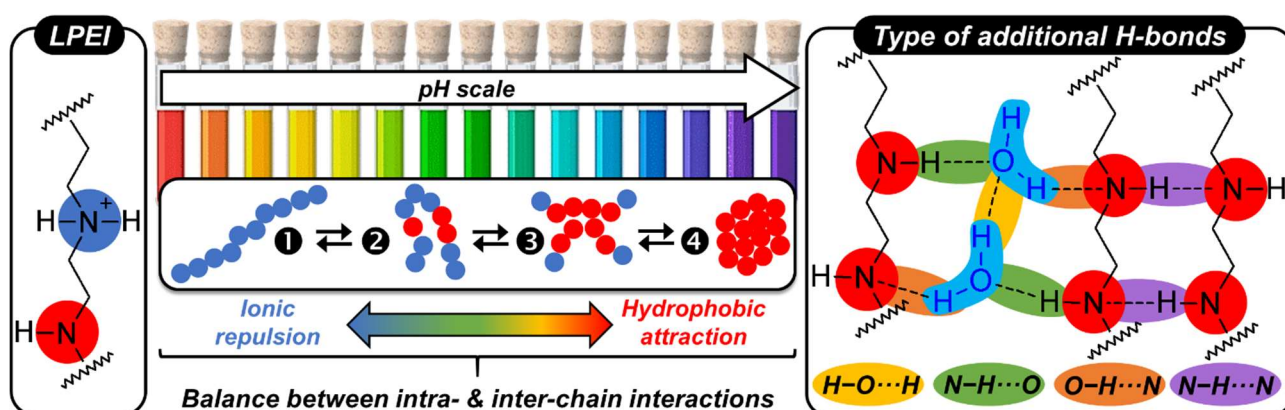

Figure 1. LPEI with adopted representations of protonated and unprotonated amine groups (left inset) and balance between intra- and inter-chain interactions as a function of pH. The right inset shows the various external and internal H-bonds between unprotonated amine groups themselves or with interstitial or superficial water molecules.

Although the aqueous behavior of LPEI presented in Figure 1 has been extensively described in the literature, particularly by Curtis *et al.* for the 2.5k Da LPEI, there is surprisingly to our knowledge no data for the 25k Da LPEI [26]. Since the understanding of the relation between the LPEI protonation and its physical state is critical for its application as Pickering emulsifier, some physicochemical properties such as conductivity (κ), pH, ζ-potential, stability index (SI, obtained by

static multiple light scattering) and hydrodynamic radius (obtained by dynamic light scattering) were investigated at 25 °C (Figure 2). All the values were measured after equilibration overnight and were plotted against initial pH, pH_{ini}, adjusted between 1 and 13 (*i.e.* pH_{ini} is the equilibrium pH value for a free LPEI solution). Consequently, all curves, presented in Figure 2, are shown in the form of a dependence of the quantities measured at equilibrium in aqueous solutions after contact with 0.1 wt.% of LPEI (25k Da) *versus* the initial pH of these solutions. For instance, pH_{eq} is defined as the pH value of an aqueous solution that is in equilibrium with the dissolved and/or the solid LPEI (Figure 2B).
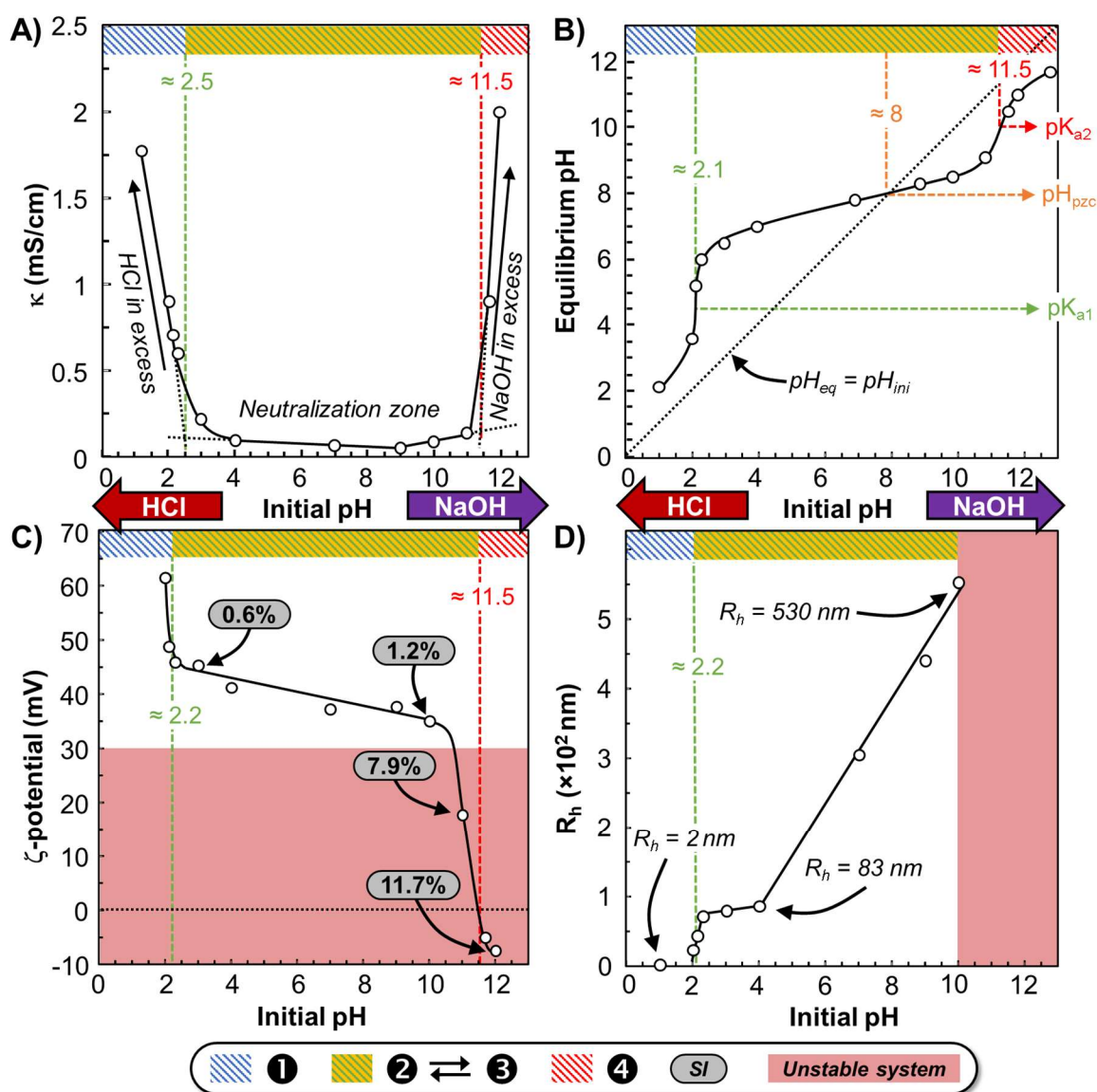

Figure 2. Conductivity (**A**, $\kappa \pm 2\%$), equilibrium pH (**B**, $pH_{eq} \pm 2\%$), ζ-potential and stability index (SI) at 30 min (**C**, $\zeta \pm 10\%$ and SI $\pm 4\%$), and hydrodynamic diameter (**D**, $D_h \pm 7\%$) plotted against the initial pH for LPEI aqueous solutions or dispersions (0.1 wt.% in water).

From a general point of view, the conductivity of aqueous LPEI solutions or suspensions can be expressed as the sum of contributions of all charged component. However, the charged LPEI (free and/or aggregated and the counter ions which condenses around it) moves more slowly than free H^+, Cl^-, Na^+ and OH^- in a given electric field: it can be assumed that the charged LPEI, whatever its physical state, does not contribute to the solution conductivity. Consequently, the κ profile (κ *vs.* pH_{ini}, Figure 2A) shows three quasi-linear segments: the first one corresponds to the HCl in excess ($pH_{ini} < 2.5$), the second one to neutralization zone due to protonation and deprotonation of the amine groups ($2.5 < pH_{ini} < 11.5$) and the third one to the excess of NaOH ($pH_{ini} > 11.5$). The two pH values found by intersection of the three lines correspond to transitions according to the protonation level of LPEI. Indeed, for solutions of pH < 2.5, since the H^+ concentration is in excess, the most abundant species is the highly protonated and soluble free LPEI (❶). At $pH_{ini} > 11.5$, enough base has been added to completely neutralize the protonated LPEI leading to a total collapse with the formation of aggregated LPEI (❹). Between these two specific pH values, it can be assumed that moderately protonated species are dominant, leaving a balance between folded and partially aggregated LPEI (❷ ⇆ ❸). It is noteworthy that the LPEI is completely dissolved in aqueous solution at $pH_{ini} < 2.3$. However, for higher pH, dispersions are observed as revealed by the systematic increase of turbidity with pH, suggesting the formation of folded LPEI and then the growth of structures by association. Indeed, LPEI undergoes a self-assembly process explained by the protonation of LPEI chains and their ability to undergo conformational and morphological transitions (see Figure 1) [27].

The pH profile (pH_{eq} *vs.* pH_{ini}, Figure 2B) provides important information about what is occurring in aqueous solution during the variation of pH_{ini} and on the identity of species present. Indeed, there are two sudden pH rises at 2.1 and 11.5 that are clearly in good agreement with the transitions detected by the κ profile (Figure 2A). The observed pH_{eq} at the two midpoints of transitions may be attributed to the pK_a values of LPEI due to the presence of two "kinds" of protons depending on whether the LPEI is free or aggregated: the first value of 4.5 is ascribed to the protons of the free solvated species

($\bullet$ is the abundant species in acidic regime) whereas the second pK_a of 10 is assigned to the protons of the aggregated LPEI ($\bullet$ is the abundant species in basic region, see above). Similar pK_a values have been reported in the literature by Curtis *et al.* for the 2.5k Da LPEI [26]. From the pH_{eq} *vs.* pH_{ini} plot, it is possible to evaluate the pH at the point of zero charge (pH_{pzc}), at which the system reaches a global charge of zero. As depicted in Figure 2B, pH_{pzc} is found to be approximately 8, which indicates that the LPEI species are globally positively charged at pH < 8 and neutral at pH > 8. In addition, it also indicates that the LPEI system act as a good buffering agent because the pH_{eq} values maintaining a relatively stable condition (~6 to 8.5) whereas the pH_{ini} values of solution changing from 2.3 to 10. In this region, between the both reported pK_a values, the buffering capacity may be ascribed to the coexistence of two moderately protonated forms of LPEI: $\bullet$ and $\bullet$. As a result, in the "weak" acidic region, the $\bullet$ species buffers the removal of H^+ ions by changing its protonation while, in the "weakly" basic pH range, the partially aggregated form of LPEI ($\bullet$) releases protons.

To confirm these state changes observed on the κ and pH profiles (Figures 2A and 2B), the ζ-potential, the stability index (SI) and the hydrodynamic radius (R_h) were determined as a function of pH_{ini} (Figures 2C and 2D). All these results are discussed from the three previously determined pH regions: acid (pH_{ini} < 2.3), buffer (2.3 < pH_{ini} < 10) and basic (pH_{ini} > 10). In the first region (pH_{ini} < 2.3), below pH 2, the LPEI has reached its maximum protonation, leading to high positive ζ-potentials (*e.g.* +62 mV at pH 2). In addition, R_h exhibits a minimal value close to 2 nm at pH 1. This value appears to be in good agreement with the radius of gyration and the experimental R_h reported in the literature for LPEI (~2-4 nm) [26,28]. As pH is raised further, the protons are removed and a sharp transition appears between pH 2 and 2.3. The ζ-potential rapidly decreases until reaching an average surface charge of +46 mV at pH 2.3. The R_h values increase rapidly, suggesting that the free LPEI ($\bullet$) is brutally converted in folded LPEI ($\bullet$) due to the decrease of electrostatic repulsions. In the second zone (2.3 < pH_{ini} < 10), the R_h increases steadily between pH 2.3 and 4 (69 and 83 nm, respectively, see Figure 2D) due to the intra-chain attraction leading to folded LPEI in order to minimize the contact with water [28]. Above pH 4, R_h sharply increases from 83 to 530 nm between

pH 4 and 10, respectively. Consequently, the folded LPEI (❷) is gradually converted to and partially aggregated LPEI (❸). In all the buffer region, the average LPEI protonation remains essentially constant as highlighted by the moderate decrease of the ζ-potential values (from +46 to +35 mV between pH 2.3 and 10). The interconversion between ❷ and ❸ suggests that these species coexist and thus explains the observed buffering capacity (see Figure 2B). In the third region (pH$_{ini}$ > 10), ζ-potential values decrease, leading to collapse and aggregation of LPEI due to insufficient electrostatic repulsions to overcome the attractive forces (*i.e.* ❹ becomes the dominant form). It is noteworthy that the hydrodynamic radii of aggregated LPEI becomes hardly detectable beyond pH 10 due to the high destabilization of the sample by sedimentation (see the SI values, for which the higher the index, the faster the sedimentation, Figure 2C). As pH is raised further, the ζ-potential decreases until reaching an average surface charge of zero at pH 11.5 (Figure 2C). This value, at which the LPEI aggregates have no net electrical charge, corresponds to the isoelectric point. As pH$_{ini}$ 11.5 matches with pH$_{eq}$ 10, the isoelectric point is in perfect agreement with the pK$_a$ value previously determined (see above). At pH > 11.5, the LPEI is fully deprotonated and a negative ζ-potential is observed (up to -7.5 mV at pH 12) due to a strong prevalence of OH$^-$ at the slipping plane (*i.e.* OH$^-$ are adsorbed on the surface of LPEI aggregates).

All these data support that the LPEI buffering capacity occurs due to continuous change between ❷ and ❸ forms, stalled among two discontinuous states (❶ and ❹). The 25k Da LPEI behaves like the 2.5k Da, previously studied by Curtis *et al.* but with much sharper transitions due to longer chain length which amplifies the phenomena of aggregation or solubilization [26]. *NB.* In the following discussion, the pH$_{eq}$ values were used instead of the pH$_{ini}$ because they are in fact more representative of the real pH of the system. Therefore, the transitions are observed at the two pK$_a$ values (4.5 and 10.5) for aqueous LPEI solution (0.1 wt.%).

3.2. Effect of pH and temperature on the physical state of LPEI in aqueous solution.

The melting and gelation temperatures have been determined for different pH values. The results are presented in Figure 3 as temperature-pH diagrams for two LPEI concentrations (0.1 and 1 wt.%). Note that the pH used here is the one acquired by the system (*i.e.* pH_{eq}, see above). From a general point of view, the two diagrams are relatively similar. Indeed, when the pH is very low, the highly charged LPEI is easily solubilized in water and temperature shows no effect on these samples. However, the transition pH for solubilisation is strongly concentration-dependent. Indeed, at 25 °C, the solubilisation is achieved for observed pH values below 5.3 and 3.7 for systems charged with 0.1 and 1 wt.% of LPEI. In other words, the solubilisation occurs at lower pH when the LPEI concentration is increased suggesting that LPEI chains are less solvated and more compacted due to the proximity of highly charged chains promoting inter-chain repulsions. In contrast, for higher pH values, two temperature-dependent transitions are clearly observed: a critical gelation temperature (CGT, below which the LPEI/water system is completely gelled) and an upper critical solution temperature (UCST, above which the LPEI is completely water-miscible) [29]. It is noteworthy that the UCST is in good agreement with the literature value (~60 °C) [30].
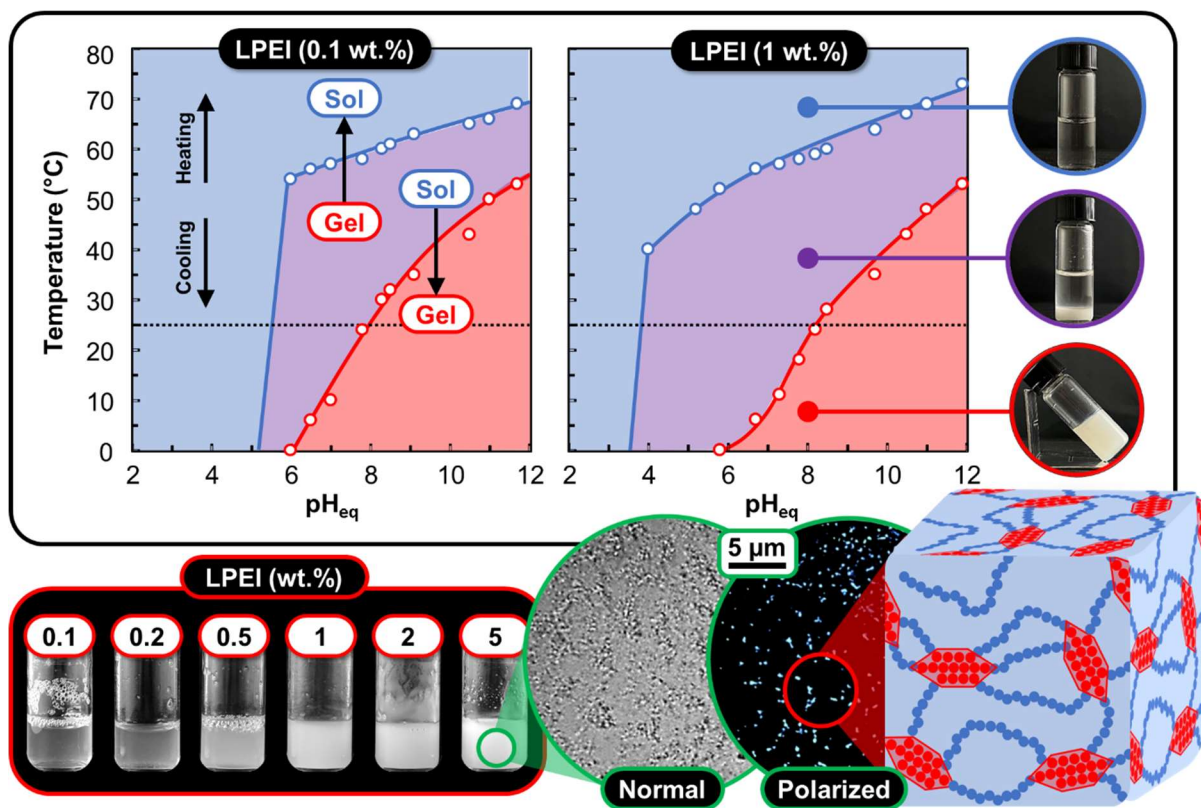
Figure 3. Temperature *versus* pH_{eq} phase diagram of LPEI aqueous samples. The gelation line depends on cooling conditions (1 °C/min, here). In the concomitant gel-sol area (purple) and on cooling, a whitish milky system is observed due to the presence of pseudo-crystalline structures in suspension (local gelation). The insets show the hydrogels as a function of the LPEI concentration (left), a typical microscopic texture under normal and polarized light, and the corresponding interpretation for the 5 wt.% LPEI hydrogel at 25 °C and $pH_{eq} \approx 8$ (right).

Although the UCST and CGT transition lines depend on cooling or heating conditions, a concomitant "gel-sol" area is observed between these both transitions. Indeed, on cooling conditions, the initial clear and homogeneous LPEI solution becomes, below the CGT, a whitish milky system in which the gel does not form an infinite network (at least within the timescale of the experiment) but rather pseudo-crystalline LPEI structures partially gelled in suspension. In contrast, on heating conditions, the gel is maintained until reaching the USCT. The concomitant "gel-sol" area is wider in acidic than in basic region due to the competition between intra- and inter-chain interactions. Indeed, for the most charged LPEI chains, the intra- and inter-chain electrostatic repulsions facilitate the LPEI solubilisation during heating and prevent the gelation during cooling. In contrast, at high pH, the uncharged LPEI is strongly aggregated (or crystallized) due to its linear structure and to the formation of H-bonds between the LPEI chains themselves (*e.g.* N−H···N) and between the LPEI and water (O−H···N and N−H···O) [24]. Therefore, in aqueous solution, LPEI leads to the formation of hydrogels after heating/cooling cycle due to this pseudo-crystallization driving mainly from H-bonds. Indeed, the microstructures of the hydrogels, examined by optical microscopy, reveal the presence of LPEI pseudo-crystalline domains in the mixture (see the right inset in Figure 3). Under polarization, this same sample reveals birefringent domains (crystallites) attached to each other by disordered regions (see Figure 3). These domains act as physical 3D cross-linked networks alongside LPEI chains not crystallized. This arrangement is highly compatible with the experimental data reported by Chatani *et al*. [31-33]. Indeed, IR and XRD studies have shown that hydrogel LPEI systems consist

of a crystalline structure at room temperature [30]. In these structures, an extended 3D network of LPEI chains in a "zigzag" conformation connected together by H-bonds was observed. However, the H-bond network is formed *via* water molecules between the LPEI chains. Indeed, each ethyleneimine unit is surrounded closely by two water molecules each linked to other LPEI chains. On heating conditions, the LPEI chains adopt random and disordered coil shape leading to the destruction of the physical hydrogel. For a given pH, as the LPEI concentration increases, the crystallized fraction becomes larger and the hydrogels change from slightly turbid to completely opaque and viscous (see the left inset in Figure 3). It is noteworthy that the real crystallite size in hydrogel is likely smaller than that show in Figure 3 due to the formation of transformation twins due to a change in crystal system during cooling. Additionally, crystal apparent stacks can be observed due to the specificity of transmitted light microscopy (sample thickness and microscope resolution).

To study the rheological behavior of LPEI hydrogels, the dependency of the viscosity on the applied shear rate is reported for various LPEI concentrations (Figure 4A). These flow curves are one of the most common characterization techniques used for determining the hydrogels tendency to flow. It is noteworthy that our hydrogels are non-Newtonian (viscoelastic) fluids with shear-thinning behavior attributed to the microstructure of gels (see Figure 4). This behavior of being highly viscous at low shear rates and exhibiting low viscosity at high ones can be beneficial in their applications such as drug delivery and injection [34]. Next, the flow curves are used to compare the viscosity of hydrogels made with various LPEI concentrations.
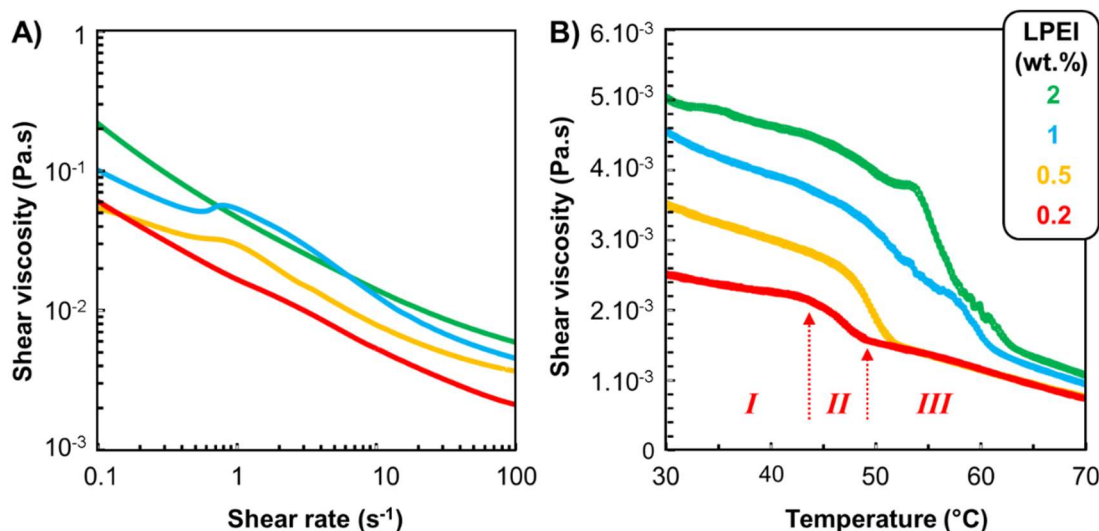
Figure 4. Shear viscosity as a function of shear rate at 25 °C and $pH_{eq} \approx 8$ (flow curves, **A**) and shear viscosity as a function of temperature at 100 s^{-1} (**B**) for LPEI hydrogels at different concentrations. The regions *I*, *II* and *III* are only presented for the 2 wt.% LPEI hydrogel.

As depicted in Figure 4A, the viscosity of hydrogels globally increases as a function of their LPEI concentration because higher shear rate is needed to induce flow. Therefore, the spreading is better for weak LPEI concentrations. It is noteworthy that the 0.5 and 1 wt.% LPEI hydrogels exhibit a transient Newtonian region in the 0.5 - 1 s^{-1} shear rate range. The Newtonian plateau indicates yield stress behavior related to a strong and rigid network structure. The sliding of the pseudo-crystalline structures over each other is limited by friction. Consequently, the network must reorganize in order to flow and the time taken to rearrange the structure is higher than the acquisition time. Obviously, at low PEI concentration (*i.e.* at 0.2 wt.%), the amount of pseudo-crystalline structures in hydrogels is reduced, resulting in the loss of the Newtonian plateau. In contrast, the absence of the Newtonian plateau at 2 wt.% LPEI concentration may be correlated with the presence of numerous pseudo-crystalline structures which can be more oriented facilitating their sliding and thus the hydrogels flow. Next, the temperature effect on the shear viscosity (at a fixed shear rate of 100 s^{-1}) is used to characterize the structure of hydrogels made with various LPEI concentrations (Figure 4B). The temperature sweep test reveals that, throughout the tested temperature range (30-70 °C), the viscosity has negative slopes for all hydrogels; however, the slope values disclose three regions. In the first

region, the slope is low, before becoming steep and more pronounced in the second one, and reaching viscosities close to those of water in the third one (***I***, ***II*** and ***III*** for LPEI 0.2 wt.%, see Figure 4B). The first region (***I***) indicates a relative structural stability of hydrogels whereas the second one (***II***) corresponds to the UCST transitions from gels to LPEI solutions (***I*** → ***III***). The least temperature stable hydrogel is the 0.2 wt.% LPEI hydrogel, whereas the hydrogel with the highest LPEI concentration (*i.e.* 2 wt.%) is the most stable. Indeed, the temperatures at which LPEI hydrogels start to degrade are gradually increased from 44 to 55 °C. Therefore, we conclude that the presence of numerous pseudo-crystalline structures improves the stability and increase the UCST values at which hydrogels begin to break down rapidly to give homogeneous LPEI solutions.

All these results support that the LPEI aqueous system could be beneficial for applications as Pickering emulsifier. Indeed, this system offers a wide range of dispersion with buffering capacity due to the coexistence of partially protonated aggregates. After a first heat and cool cycle, these species allow the formation of hydrogels due to an adequate and spontaneous repartition of the hydrophobic and hydrophilic regions on the LPEI chains. Actually, the hydrophobic regions are able to induce a pseudo-crystallization, driven by the hydrophobic forces and by H-bonds, whereas the protonated ones remain largely solvated. The competition between the solvation and the aggregation results in the formation of a self-assembling 3D network where the crystallized hydrophobic domains act as knots. The existence of crystallites is confirmed over a wide temperature range from 0 to 50-60 °C (*i.e.* the sol-gel temperature transition), even after 10 successive heat and cool cycles. Consequently, the LPEI functions as a robust bipolar tecton with solvophilic and solvophobic regions leading to the bottom-up self-assembly of hydrogels and likely providing a good platform to obtain Pickering-like emulsions by a mechanism close to that observed from the self-assembly of α-cyclodextrin and polyethylene glycol (polar and apolar tectons, respectively) using the colloidal tectonics approach [12]. Moreover, we can predict that the LPEI crystallites should lead to stable Pickering emulsions through the formation of a steric barrier, electrostatic repulsions (*e.g.* ζ = +38 ±

4 mV at pH 8, see above) and gelation of the aqueous phase preventing aggregation and coalescence processes.

3.3. LPEI-based emulsions.

The LPEI is neither soluble in conventional organic solvents (heptane, toluene, isopropyl myristate and liquid paraffin) nor in vegetable oils (corn, sunflower, olive and castor oil). Nevertheless, by screening a series of water/oil biphasic systems (1:1 w/w) in the presence of LPEI (0.5 wt.%), we obtained whitish emulsions after homogenization at 11,500 rpm during 60 s at 25 °C (note that the olive oil emulsion is yellowish). Typically, the solid/liquid contact angles (θ) to a surface of a droplet can be used to characterize the hydrophilicity or hydrophobicity of particles and predict the emulsion type. Indeed, if the testing solvent is water, we have "hydrophilic" and "hydrophobic" particles for θ < 90° and θ > 90°, respectively (the opposite holds for organic solvents). More specifically, O/W and W/O emulsions are obtained with hydrophilic and hydrophobic particles, respectively. The phase with the better wetting capacity on the particles becomes the continuous phase, while the other becomes the dispersed phase. In our case, θ are not measurable. Indeed, after the spreading of a liquid (water or *n*-heptane) on the compressed LPEI particles of, the solvent rapidly penetrates inside the solid. It is noteworthy that this problem cannot be overcame with more viscous solvents such as paraffin oil, or none of the other solvents mentioned in Table 1. Nevertheless, the high electrical conductivity of these emulsions indicates an aqueous external phase. Therefore, the LPEI stabilizer has more affinity for water than oils.

Table 1. Emulsion fraction and log-normal parameters used to fit the droplet size distribution (median diameter, d_m, skewness factor, ω, and amplitude, A) versus time for O/W emulsions at 25 °C.[a]

Oil	Emulsion fraction (v/v)		Droplet size distribution parameters at 24h[b]		
	0h	24h	d_m (μm)	ω	A
Heptane	100	100	38	0.41	428.4
Toluene	100	78	10	0.76	243.6

Isopropyl myristate	100	81	7	0.26	44.7
Liquid paraffin	100	79	1	0.40	74.5
Corn	100	77	1	0.56	35.9
Sunflower	100	91	1	0.53	55.3
Olive	100	54	1	0.50	26.4
Castor	100	87	1	0.54	45.8

[a] Conditions: 0.5 wt.%, LPEI, 49.75 wt.% water and 49.75 wt.% oil, 11,500 rpm, 60s, 25 °C. [b] Obtained with log-normal function with OriginPro 8® , USA (see Eq. 1).

The stability of these emulsions has been examined by the change in emulsion volume fraction as a function of storage time at 25 °C. At the initial time, the emulsion volume fraction is 100% (v/v) for all emulsions (Table 1). Unfortunately, a destabilization process is observed within 24 hours for all emulsions except with heptane. In spite of everything, a slight destabilization appears after 48h for the latter. Next, the individual droplet diameters were obtained from the micrographs recorded after 24h using ImageJ. As right-skewed data were obtained, a log-normal function, F(d), was used to fit the distribution using three parameters (see Eq. 1).

$$F(d)=A/(\sqrt{2\pi}\omega d) \times \exp\left(-\left(\ln(d/d_m)\right)^2/2\omega^2\right) \qquad (1)$$

where A is the amplitude, ω is the skewness factor, d is the measured droplet diameters, and d_m is the median diameter. By using the least-squares fitting procedure, the three log-normal parameters are reported in Table 1. After 24 h, the average droplet sizes depend on the oil used: heptane provides the largest droplets while the smallest ones are obtained with liquid paraffin, corn, sunflower, olive and castor oils (38 *vs.* 1 μm). Presumably the difference in droplet size results from the greater or lesser ability of the solvent to interact with the LPEI crystallites (see above). The instability of all Pickering emulsions after 24h (expect with heptane) is due to the wetting capacity of the particles (reflected by solid/liquid contact angles, θ, see above). As previously mentioned, the phase with the better wetting capacity on the particles becomes the continuous phase, while the other becomes the dispersed phase. As all emulsions are of O/W-type, the LPEI stabilizer are hydrophilic. However, more stable Pickering emulsions are obtained when the contact angle is close to 90°, where the particles are well-balanced between the two phases. If θ is away from 90°, the particle will be less

likely to prevent the coalescence of the droplets. Unfortunately, as θ are not measurable (see above), it is not possible to validate this assumption. Finally, all ω values are comprised between 0.26 and 0.76. When the skewness (ω) goes to zero, the log-normal distribution tends to a normal distribution, so the distribution of toluene-based emulsion is significantly more right-skewed than that of isopropyl myristate. In other words, the toluene-based emulsion is the most polydisperse system.

Although LPEI provides emulsions with various oils, paraffin was chosen because they have the best compromise between median droplet size and polydispersity. Nevertheless, as the optimal composition, leading to stable emulsion, is not known, the stabilization/destabilization mechanisms have been investigated. The optical microscopy of the paraffin-based emulsion stabilized by 0.5 wt.% LPEI shows the presence of crystallites in the form of needles or rods located at the droplet surface (Figure 5A). It is noteworthy that the crystallites participate in the emulsion stabilization because polarized light coming from the surface of droplets (see Figure 5A). However, the real crystallite size at the droplet surface is probably smaller than that show in Figure 5 due to the formation of deformation or gliding twins resulting of stress on the crystal formed during the emulsification at 11,500 rpm with a rotor-stator. Additionally, crystal apparent stacks can be observed due to the specificity of transmitted light microscopy (see above). Next, multiple light scattering was performed to provide real-time information on the destabilization processes. To facilitate data analysis, backscattering profile at 0h was used as a baseline and were subtracted from the profiles at other times. The ΔBS profile of paraffin-based emulsion stabilized by 0.5 wt.% LPEI is shown in Figure 5B.
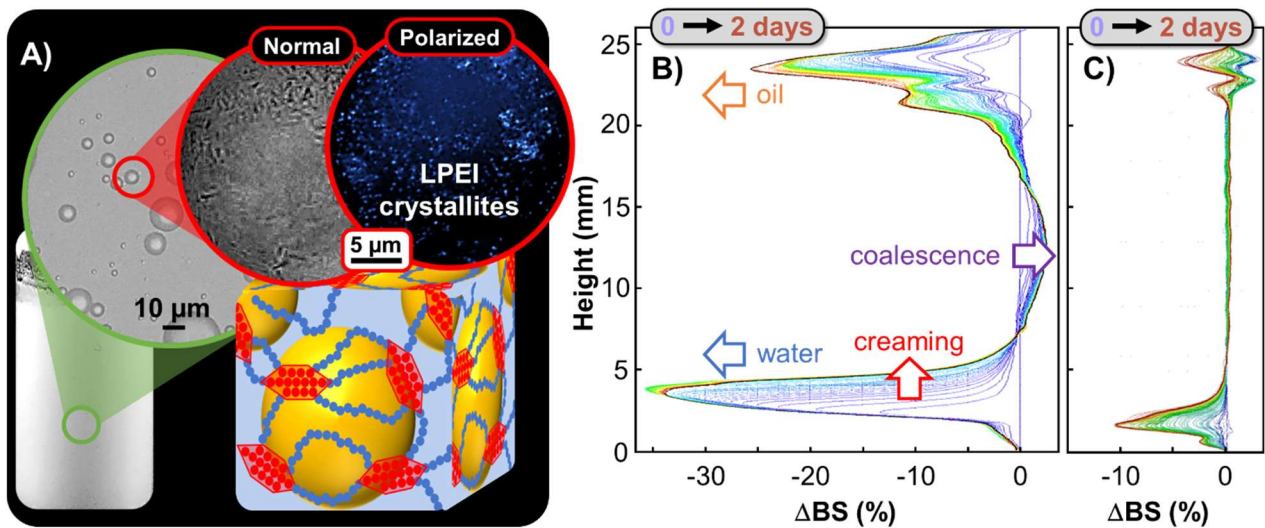
Figure 5. Macroscopic and microscopic (under normal and polarized light) views of paraffin-in-water emulsions stabilized by 0.5 wt.% LPEI with interpretation (**A**) and backscattering (ΔBS) versus sample height and time at 25 °C for 0.5 and 2 wt.% LPEI emulsions (**B** and **C**, respectively).

As shown in Figure 5B, the ΔBS values decreased at both bottom and top of the sample while they increased in the middle part over time. The decrease of ΔBS signals is attributed to the appearance of an upper oily and lower aqueous phases, which can be detected by the naked eye. Therefore, the destabilization process is induced simultaneously by both creaming and coalescence of the dispersed oil droplets. With the increase of time, the droplets migrate from the bottom to the top of the emulsion, leading to a clear lower aqueous phase, *i.e.* creaming responsible for a phase separation between the emulsion and the continuous phase. During this time, the oil droplets coalesce, leading to the appearance of an upper oil phase. Coalescence is significantly more undesirable than creaming because it is responsible for emulsion destruction and phase separation between the continuous and dispersed phases. As Pickering stabilization is supported by the adsorption of LPEI crystallites onto the droplets surface (Figure 5A), it can be assumed that the coalescence is limited. Indeed, for Pickering emulsions, the droplets will coalesce when the droplets surface is insufficiently covered [1,4]. Consequently, we have increased the amount of LPEI in the system in order to achieve a more compact monolayer to prevent the droplets from coalescing, which should make the emulsion more stable. As expected, a significant variation of ΔBS profile is observed for the emulsion stabilized by

2 wt.% LPEI (compare Figures 5B and 5C). Indeed, the creaming process is clearly less important and coalescence is almost absent, indicating that the addition of additional LPEI helps to further stabilize emulsion. Unlike the emulsion stabilized with 0.5 wt.% LPEI, the 2 wt.% one exhibits long-term stability, since no macroscopic phase separation cannot be detected by the naked eye after 4 months. Again, these findings support that the emulsion is stabilized by LPEI crystallites.

In spite of everything, as the emulsion stabilization may result from the combination of the absorbed crystallites and/or of the gelation of the continuous phase, the rheological properties were studied by applying the same conditions as those used for the hydrogels (Figure 6).
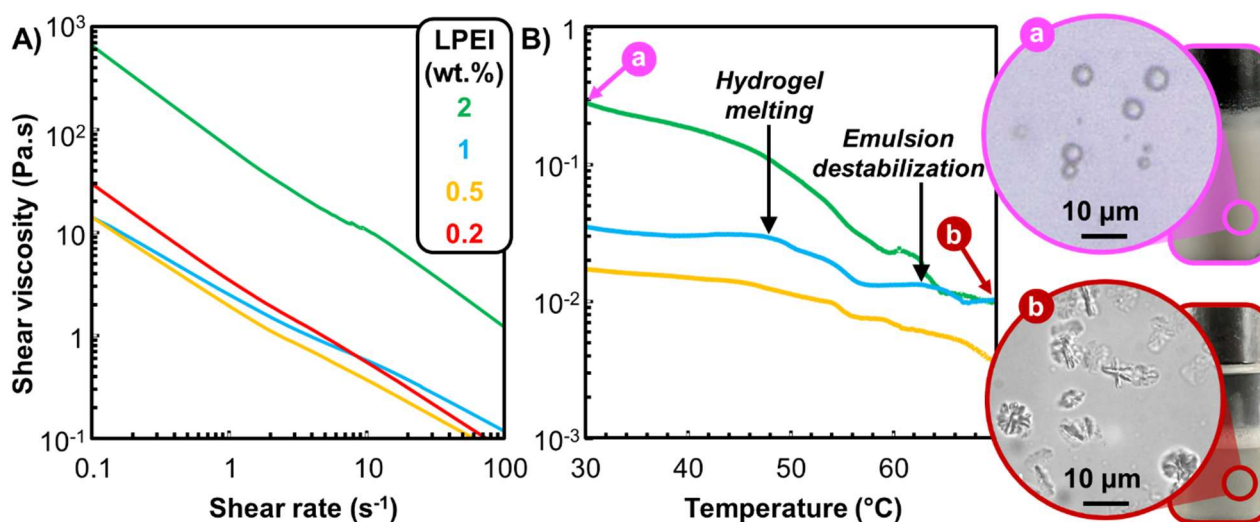

Figure 6. Shear viscosity as a function of shear rate at 25 °C (flow curves, **A**) and shear viscosity as a function of temperature at 100 s^{-1} (**B**) for paraffin-in-water emulsions stabilized by at different LPEI concentrations. The insets show the macroscopic and microscopic observations of 2 wt.% LPEI emulsions at 30 and 70 °C (**a** and **b**, respectively).

All emulsions are, on average, a hundred times more viscous than hydrogels (compare Figures 4A and 6A). Nevertheless, the viscosities of emulsions stabilized by 0.2, 0.5 and 1 wt.% of LPEI are of the same order of magnitude in the investigated shear rate range. As the 2 wt.% emulsion exhibits long-term stability due to the absence of coalescence, the proportion of oil-water interface covered by the LPEI crystallites is probably close to a compact monolayer (see above). If the LPEI crystallites

amount decreases, the proportion of oil-water interface covered by the particles is partial and coalescence occurs. Consequently, we can suppose that the emulsions stabilization is the combined result of the absorbed crystallites and/or of the gelation of the continuous phase. Both stabilizations occur for high LPEI concentration but the hydrogelation is predominant in weak concentration range. Next, the temperature effect on the shear viscosity (at a fixed shear rate of 100 s^{-1}) is used to distinguish hydrogel melting and emulsion destabilization (Figure 6B). From a general point of view, the thermal stability of emulsions is significantly improved with the increase of LPEI concentration. Although, for all emulsions, viscosity decreases with the increasing temperature, irregularities are observed. For instance, the emulsion stabilized by 1wt.% LPEI present two successive viscosity drops at 48 and 63 °C. The first transition is attributed to the hydrogel melting and the second one to the emulsion destabilization. Furthermore, the more the concentration is increased, the more pronounced the transitions, but the more it is decreased, the softer they are. Consequently, hydrogel melting does not mean emulsion destabilization. It can be assumed that the LPEI crystallites located at the interface of the droplets solubilize at a higher temperature than the hydrogel leading to the two successive transitions. Obviously, LPEI crystallites concentration influences both the rheological properties and stability of emulsions: at low concentration, the emulsions have better fluidity and weak stability, whereas at high concentration, they have stronger gel-like structures leading to long-term stability. It is noteworthy that, at high temperature, the emulsion destabilization occurs by complete dehydration of LPEI leading to turbid aqueous phase due to the formation of star-like crystalline structures caused by multiple crystal twinning at the onset of growth (see Figure 6). As these structures do not exist for hydrogels that exhibit an upper critical solution temperature, above which the LPEI is fully miscible with water, we can suppose that the LPEI co-crystallizes with the paraffin molecules with increasing temperature.

To ascertain the higher-order structure of these emulsions in further detail, dynamic viscoelasticity measurements were carried out**Figure 7**. Frequency dependence of G' and G'' for paraffin-in-water emulsions using different LPEI concentrations.. Figure 7 shows the variation of G' (storage modulus)

and G' (loss modulus) as a function of the frequency. All the emulsions reveal a typical gel-like structure (G' > G'') in the linear viscoelastic region (0.1-10 Hz). Furthermore, G' and G'' values were increased with rising LPEI concentration over the entire frequency range, indicating that the gel strength of the emulsions was positively related to the LPEI concentration. This behavior reflects the superior physical stability of the emulsions formed due to the gelation of the aqueous continuous phase. As the emulsion stabilized with 2 wt.% LPEI shows the highest apparent viscosity over the entire shear rate range (see Figure 5A), it exhibits the most compact microstructure and the strongest mechanical performance. Thus, even if LPEI crystallites are adsorbed at the water/oil interface, the gelation of the continuous phase also prevents the droplets from coalescing, making this emulsion more stable.
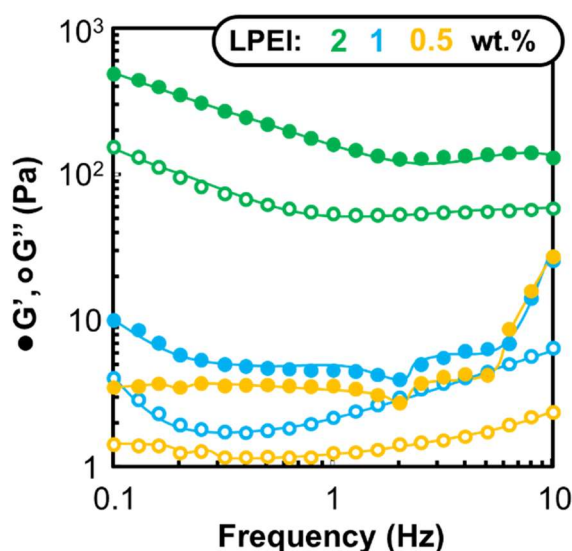

Figure 7. Frequency dependence of G' and G'' for paraffin-in-water emulsions using different LPEI concentrations.

Consequently, LPEI forms long-term stable emulsions with typical gel-like and shear-thinning behavior. Nevertheless, stabilizing mechanism is unusual. Indeed, the LPEI alone ensures an emulsifying effect both by hydrophilic protonated and hydrophobic self-aggregated (crystallites) parts. At low LPEI concentrations, the crystalized regions act as knots and contribute to the gelation of the aqueous continuous phase and to the emulsions stability. However, when the LPEI

concentration is increased, crystallites also distribute homogenously on the droplets surface, leading to Pickering-like stabilization.

3.4. Reversibility of Pickering emulgels.

The as-prepared Pickering emulgels could provide reversible systems with high degree of control due to their self-assembled nature. Indeed, our physicochemical results support that the destructuring/ restructuring of emulsions could easily be achieved by temperature or pH changes because high temperature or acidic medium alters the hydrophilic and hydrophobic sections leading to inadequate stabilization by modifying the gelation of the aqueous continuous phase as well as the Pickering-like stabilization (see above). Firstly, the thermo-reversibility of the 2 wt.% LPEI emulsion was probed. In particular, after the first emulsification at 11,500 rpm during 60 s at 25 °C (see run 1 in Figure 8), the emulsion was destabilized by heating at 75 °C. The separated system was simply re-emulsified in similar condition after cooling at 25 °C to obtain a new emulsion (see run 2 in Figure 8). The responsive emulsions were successfully reformed over 10 consecutive runs, and the emulsion volume fraction was similar and more than 95% in each case (Figure 8). The weak decrease of emulsion fraction can be related to the formation of star-like crystalline structures between the LPEI and oil molecules by hydrophobic interactions, which would prevent the formation of a new Pickering emulgel (see inset b in Figure 6). Nevertheless, this result suggested that the LPEI emulsion can easily be stabilized and destabilized without additional treatment such as centrifugation.
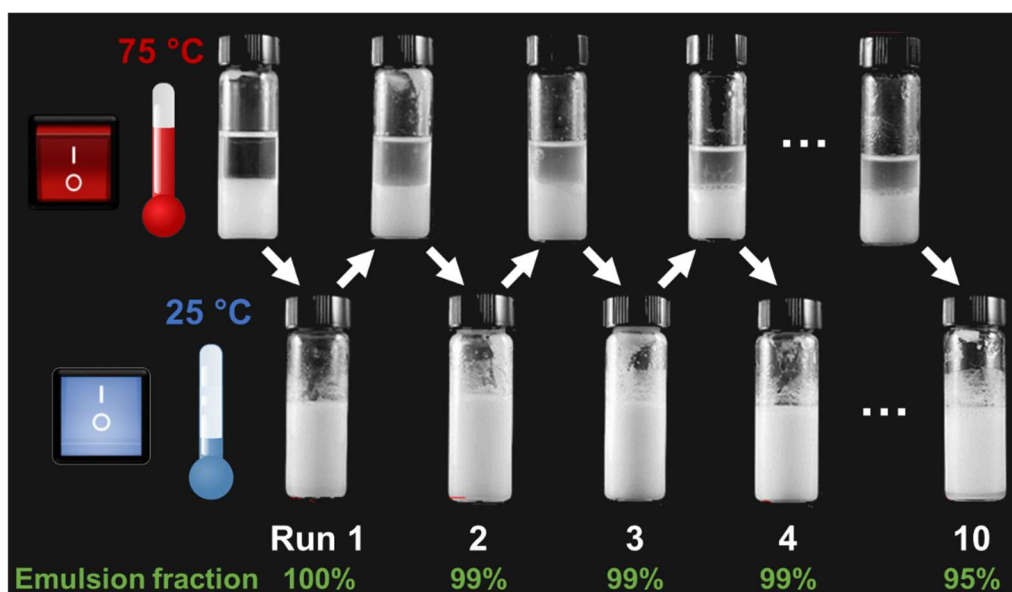
Figure 8. Thermo-reversibility of paraffin-in-water emulsions stabilized by LPEI (49/49/2 wt.%, 11,500 rpm, 60 s) with emulsion volume fraction over 10 runs.

Finally, the recyclability of the 2 wt.% LPEI emulgel platform was tested by cycling pH between 8 and 5. After the first emulsification at pH 8, the emulsion was partially broken by decreasing the pH at 5 at ambient temperature. The phase separation was fully obtained after centrifugation. The emulsion was restored by addition of NaOH until reaching pH 8, followed by stirring as described previously, and this process was performed over 3 consecutive runs (Figure 9). Unfortunately, we failed to construct highly recyclable pH-responsive emulsions since the emulsion volume fraction decrease up to 93% after the third run. Compared with the previous method, this pH switchable strategy needs centrifugation to achieve complete phase separation and the pH changes results in ionic strength variations. As the pH-reversibility is due to the greater hydrophilicity of protonated LPEI at low pH and the greater hydrophobicity of neutral LPEI leading to polymer aggregation, the ionic strength variations impact the re-emulsification. For instance, after 10 consecutive runs, the emulsion totally disappears due to inadequate hydrophilic/hydrophobic ratio on the LPEI.
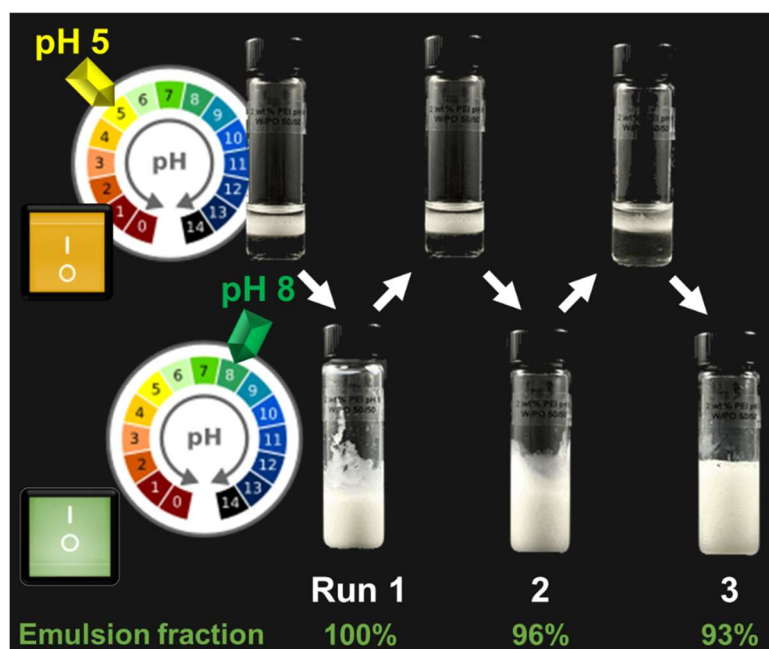
Figure 9. Alternating stabilization and phase separation by pH trigger of paraffin-in-water emulsion stabilized by LPEI (49/49/2 wt.%, 11,500 rpm, 60 s) with emulsion volume fraction over 3 runs.

4. Conclusions

In this study, according to the colloidal tectonic concept, we have developed a new strategy to obtain "on-off" Pickering-like emulsions from linear polyethyleneimine (LPEI, 25k Da). This polymer, with an intrinsically hydrophobic backbone, can be easily protonated to adjust its charge density. In aqueous solution, depending on its protonation, the polymer is in free form (pH < 2.3) or aggregated (pH > 10). Between these two behaviors, LPEI acts as a buffering agent by continuous protonation/deprotonation of the amine groups. As a result, highly charged and neutral sections co-exist, leading to reversible and dynamic bipolar regions. After a first heat and cool cycle, at neutral pH, the adequate and spontaneous distribution of hydrophobic and hydrophilic sections leads to hydrogels by formation of a 3D network where the crystallized hydrophobic domains act as knots linked by the charged segments. In the presence of various oils, the hydrogels provide long-term stable emulsions with typical gel-like and shear-thinning behavior. LPEI ensures emulsifying and stabilizing effects both by the adsorption of crystallites onto the droplets surface and the gelation of the aqueous continuous phase, leading to Pickering emulgels by self-assembly. These systems are

reversible and their dynamics is an inherent and essential property leading to stability that can be affected by external stimuli (up to 10 consecutive runs). Nevertheless, contrary to the accepted rules which claim that at least two tectons of opposite polarity are required and that one of them must have a rigid structure [12], we have clearly demonstrated that a single self-complementary polymer-based tecton can be used to design supracolloidal systems. The polymer must be of high molecular weight to obtain balanced properties between solvophilic and solvophobic requirements generating those of rigidity and flexibility. Compared to conventional Pickering emulsions [18-23], LPEI raw material is inexpensive, commercially available and can be used without any chemical transformation, providing very simple and cheap responsive emulsions. In addition, LPEI-based emulgels are in line with the current trend of simplifying formulas in term of ingredients since they are obtained with a single tecton, unlike the other systems based on the colloidal tectonics approach [6,7,12,13,35-51]. Conceptually, as LPEIs with other molecular weights can be used to stabilize these Pickering emulgels, works are currently underway to extend the scope of single tecton colloidal tectonics approach. From a more practical standpoint, these responsive emulsions are very attractive to perform chemical transformations in biphasic media with significant environmental and economic perspectives [47]. Indeed, after reaction, pH or temperature can be adjusted to allow rapid phase separation and easy recovery of the LPEI particles [52]. On the other hand, the high molecular weight LPEIs are known to increase cytotoxicity due to their ability to bind to the cell surfaces and disrupt their membranes [16]. As their biocidal mechanism is very close to that of quaternary ammonium compounds (QACs), widely used in healthcare systems to prevent and control infections, works are under investigation to evaluate the biocidal activity of LPEI (25k Da) emulgels [53]. Furthermore, these formulations are of potential interest to prevent the spread not only of bacterial diseases but also of viral ones. Indeed, the severe acute respiratory syndrome coronavirus 2 (SARS-CoV-2) that causes coronavirus disease (CoViD), is an enveloped virus, meaning that the viral capsid is surrounded by a lipoprotein layer and that the outer wrapping helps the virus survive and infect host cells [6,53]. Therefore, LPEI-based emulgels could be highly helpful to obtain broad-spectrum biocidal and

virucidal formulations for the chemical disinfection of surfaces and/or hospital devices to avoid the spread of infectious diseases and the use of conventional QACs. For instance, on 629 disinfectants, approved by Health Canada, 343 use QACs [54]. These ammonium-based formulations, evacuated "down-the-drain", have environmental hazards because the bioavailable fraction of quaternary ammoniums in environmental waters is estimated around 5% [55]. In this context, the easy control of the emulgels creates a particular exciting solution to facilitate the phase separation and the fully recovery of toxic LPEI by filtration in wastewater treatment plants. Nevertheless, the use of this formulation in the fight against viruses remains inconclusive until data is available on its efficacy and safety. Therefore, the authors does not advice the use of LPEI in any forms for disinfection of contaminated surfaces. However, in the current pandemic situation, all these facts, encouraging us to investigate these LPEI-based emulsions not only against bacteria and fungi but also against viruses, including SARS-CoV-2.

CRediT authorship contribution statement

Grégory Douyère: Methodology, Investigation, Writing. Loïc Leclercq: Conceptualization, Formal analysis, Writing. Véronique Nardello-Rataj: Conceptualization, Supervision, Funding acquisition, Project administration, Writing, Validation.

Declaration of competing interest

The authors declare that they have no known competing financial interests or personal relationships that could have appeared to influence the work reported in this paper.

Acknowledgements

References

[1]   Y. Yang, Z. Fang, X. Chen, W. Zhang, Y. Xie, Y. Chen, Z. Liu, W. Yuan, An overview of Pickering emulsions: solid-particle materials, classification, morphology, and applications, Front. Pharmacol., 8 (2017) 287. DOI: 10.3389/fphar.2017.00287.

[2]   T. Zhang, J. Xu, J. Chen, Z. Wang, X. Wang, J. Zhong, Protein nanoparticles for Pickering emulsions: A comprehensive review on their shapes, preparation methods, and modification methods, Trends Food Sci. Technol., 113 (2021) 26-41. DOI: 10.1016/j.tifs.2021.04.054.

[3]   Abdullah, J. Weiss, T. Ahmad, C. Zhang, H. Zhang, A review of recent progress on high internal-phase Pickering emulsions in food science, Trends Food Sci. Technol., 106 (2020) 91-103. DOI: 10.1016/j.tifs.2020.10.016.

[4]   C. Albert, M. Beladjine, N. Tsapis, E. Fattal, F. Agnely, N. Huang, Pickering emulsions: Preparation processes, key parameters governing their properties and potential for pharmaceutical applications, J. Control. Release, 309 (2019) 302-332. DOI: 10.1016/j.jconrel.2019.07.003.

[5]   J. Tang, P.J. Quinlan, K.C. Tam, Stimuli-responsive Pickering emulsions: recent advances and potential applications, Soft Matter, 11 (2015) 3512-3529. DOI: 10.1039/c5sm00247h.

[6]   L. Leclercq, J. Tessier, V. Nardello-Rataj, A.-R. Schmitzer, Highly active, entirely biobased antimicrobial Pickering emulsions, ChemMedChem, 16 (2021) 2223-2230. DOI: 10.1002/cmdc.202100030.

[7]   L. Leclercq, V. Nardello-Rataj, Pickering emulsions based on cyclodextrins: A smart solution for antifungal azole derivatives topical delivery, Eur. J. Pharm. Sci., 82 (2016) 126-137. DOI: 10.1016/j.ejps.2015.11.017.

[8]   F. Rancan, Q. Gao, C. Graf, S. Troppens, S. Hadam, S. Hackbarth, C. Kembuan, U. Blume-Peytavi, E. Rühl, J. Lademann, A. Vogt, Skin penetration and cellular uptake of amorphous

silica nanoparticles with variable size, surface functionalization, and colloidal stability, ACS Nano., 6 (2012) 6829-6842. DOI: 10.1021/nn301622h.

[9] R. Pinho Morais, S. Hochheim, C.C. de Oliveira, I.C. Riegel-Vidotti, C.E.B. Marino, Skin interaction, permeation, and toxicity of silica nanoparticles: Challenges and recent therapeutic and cosmetic advances, Int. J. Pharm., 614 (2022) 121439. DOI: 10.1016/j.ijpharm.2021.121439.

[10] J. Allana, S. Belz, A. Hoeveler, M. Hugas, H. Okuda, A. Patri, H. Rauscher, P. Silva, W. Slikker, B. Sokull-Kluettgen, W. Tong, E. Anklam, Regulatory landscape of nanotechnology and nanoplastics from a global perspective, Regul. Toxicol. Pharmacol., 122 (2021) 104885. DOI: 10.1016/j.yrtph.2021.104885.

[11] M. R. Gwinn, V. Vallyathan, Nanoparticles: health effects-pros and cons, Environ. Health Perspect., 114 (2006) 1818-1825. DOI: 10.1289/ehp.8871.

[12] L. Leclercq, Get beyond limits: from colloidal tectonics concept to the engineering of eco-friendly catalytic systems, Front. Chem., 6 (2018) 168. DOI: 10.3389/fchem.2018.00168.

[13] L. Leclercq, J.-F. Dechézelles, G. Rauwel, V. Nardello-Rataj, In vitro study of versatile drug formulations based on α-cyclodextrin and polyethylene glycol using colloidal tectonics, J. Drug Deliv. Sci. Technol., 59 (2020) 101913. DOI: 10.1016/j.jddst.2020.101913.

[14] M. Jug, B. K. Yoon, J. A. Jackman, Cyclodextrin-based Pickering emulsions: functional properties and drug delivery applications, J. Incl. Phenom. Macrocycl. Chem., 101 (2021) 31-50. DOI: 10.1007/s10847-021-01097-z.

[15] H. Jiang, Y. Sheng, T. Ngai, Pickering emulsions: Versatility of colloidal particles and recent applications, Curr. Opin. Colloid Interface Sci., 49 (2020) 1-15. DOI: 10.1016/j.cocis.2020.04.010.

[16] A. Zakeri, M. Kouhbanani, N. Beheshtkhoo, V. Beigi, S.M. Mousavi, S. Hashemi, A. Karimi Zade, A.M. Amani, A. Savardashtaki, E. Mirzaei, S. Jahandideh, A. Movahedpour,

Polyethylenimine-based nanocarriers in co-delivery of drug and gene: a developing horizon, Nano Rev. Exp., 9 (2018) 1488497. DOI: 10.1080/20022727.2018.1488497.

[17] Y. Fukuda, D. Abe, Y. Tanaka, J. Uchida, N. Suzuki, T. Miyai, Y. Sasanuma, Solution properties of poly(N-methylethylene imine), a highly hydrophilic polycation, Polym. J., 48 (2016) 1065-1072. DOI: 10.1038/pj.2016.71.

[18] M. Williams, S. P. Armes, D. W. York, Clay-Based Colloidosomes, Langmuir, 28 (2012) 1142-1148. DOI: 10.1021/la2046405.

[19] M. Williams, N. J. Warren, L. A. Fielding, S. P. Armes, P. Verstraete, J. Smets, Preparation of double emulsions using hybrid polymer/silica particles: new Pickering emulsifiers with adjustable surface wettability, ACS Appl. Mater. Interfaces, 6 (2014) 20919-20927. DOI: 10.1021/am505581r.

[20] M. Williams, S. P. Armes, P. Verstraete, J. Smets, Double emulsions and colloidosomes-in-colloidosomes using silica-based Pickering emulsifiers, Langmuir, 30 (2014) 2703-2711. DOI: 10.1021/la500219m.

[21] W. Li, B. Ju, S. Zhang, Novel amphiphilic cellulose nanocrystals for pH-responsive Pickering emulsions, Carbohydr. Polym., 229 (2020) 115401. DOI: 10.1016/j.carbpol.2019.115401.

[22] A. Wusiman, J. Li, X. Abulikemu, G. Pengfei, Z. Mai, W. Jiang, Z. Liu, D. Wang, S. Abula, Q. Guo, Polyethyleneimine modified Pickering emulsion as a novel adjuvant to induce strong and long-lasting immune responses, Int. J. Pharm., 619 (2022) 121713. DOI: 10.1016/j.ijpharm.2022.121713.

[23] K. Kolman, G. Poggi, M. Baglioni, D. Chelazzi, P. Baglioni, M. Persson, K. Holmberg, R. Bordes, pH-Controlled assembly of polyelectrolyte layers on silica nanoparticles in concentrated suspension, J. Colloid Interface Sci., 615 (2022) 265-272. DOI: 10.1016/j.jcis.2022.01.120.

[24] K. F. Weyts, E. J. Goethals, Back titration of linear polyethylenimine: Decrease of pH by addition of sodium hydroxide, Makromol. Chem., Rapid Commun. 10 (1989) 299-302. DOI: 10.1002/marc.1989.030100611.

[25] T. Hashida, K. Tashiro, Y. Inaki, Structural investigation of water-induced phase transitions of poly(ethylene imine). III. The thermal behavior of hydrates and the construction of a phase diagram, J. Polym. Sci. B: Polym. Phys. 41 (2003) 2937-2948. DOI: 10.1002/polb.10611.

[26] K. A. Curtis, D. Miller, P. Millard, S. Basu, F. Horkay, P. L. Chandran, Unusual salt and pH induced changes in polyethylenimine solutions, PLoS One, 11 (2016) e0158147. DOI: 10.1371/journal.pone.0158147.

[27] M. Jain, J. R. Seth, L. R. Hegde, K. P. Sharma, Unprecedented self-assembly in dilute aqueous solution of polyethyleneimine: formation of fibrillar network, Macromolecules, 53 (2020) 8974-8981. DOI: 10.1021/acs.macromol.0c01501.

[28] C. E. Gallops, C. Yu, J. D. Ziebarth, Y. Wang, Effect of the protonation level and ionic strength on the structure of linear polyethyleneimine, ACS Omega, 4 (2019) 7255-7264. DOI: 10.1021/acsomega.9b00066.

[29] X. Xue, L. Thiagarajan, S. Braim, B. R. Saunders, K. M. Shakesheff, C. Alexander, Upper critical solution temperature thermo-responsive polymer brushes and a mechanism for controlled cell attachment, J. Mater. Chem. B, 5 (2017) 4926-4933. DOI: 10.1039/C7TB00052A.

[30] J.-J Yuan, R.-H. Jin, Fibrous crystalline hydrogels formed from polymers possessing a linear poly(ethyleneimine) backbone, Langmuir, 21 (2005) 3136-3145. DOI: 10.1021/la0471182l.

[31] Y. Chatani, T. Kobatake, H. Tadokoro, R. Tanaka, Structural studies of poly(ethylenimine): double-stranded helical chains in the anhydrate, Macromolecules, 1982, 15, 170-176. DOI: 10.1021/ma00229a034.

[32] Y. Chatani, T. Kobatake, H. Tadokoro, Structural studies of poly(ethylenimine): structural characterization of anhydrous and hydrous states and crystal structure of the hemihydrate, Macromolecules, 1983, 16, 199-204. DOI: 10.1021/ma00236a009.

[33] Y. Chatani, H. Tadokoro, T. Saegusa, H. Ikeda, Structural studies of poly(ethylenimine): structures of two hydrates of poly(ethylenimine): sesquihydrate and dehydrate, Macromolecules, 1981, 14, 315-321. DOI: 10.1021/ma50003a017.

[34] A. Simões, M. Miranda, C. Cardoso, F. Veiga, F. Vitorino, Rheology by design: a regulatory tutorial for analytical method validation, Pharmaceutics, 12 (2020) 820. DOI: 10.3390/pharmaceutics12090820.

[35] K. Hashizaki, T. Kageyama, M. Inoue, H. Taguchi, U. Ueda, Y. Saito, Study on preparation and formation mechanism of n-alkanol/water emulsion using α-cyclodextrin, Chem. Pharm. Bull., 55 (2007) 1620-1625. DOI: 10.1248/cpb.55.1620.

[36] L. Leclercq, A. Mouret, A. Proust, V. Schmitt, P. Bauduin, J.-M. Aubry, V. Nardello-Rataj, Pickering emulsion stabilized by catalytic polyoxometalate nanoparticles: a new effective medium for oxidation reactions, Chem. Eur. J., 18 (2012) 14352-14358. DOI: 10.1002/chem.201201799.

[37] L. Leclercq, R. Company, A. Mühlbauer, A. Mouret, J.-M. Aubry, V. Nardello-Rataj, Versatile eco-friendly Pickering emulsions based on substrate/native cyclodextrin complexes: A winning approach for solvent-free oxidations, ChemSusChem, 6 (2013) 1533-1540. DOI: 10.1002/cssc.201300081.

[38] J. Potier, S. Menuel, M.-H. Chambrier, L. Burylo, J.-F. Blach, P. Woisel, E. Monflier, F. Hapiot, Pickering emulsions based on supramolecular hydrogels: Application to higher olefins' hydroformylation, ACS Catal., 3 (2013) 1618-1621. DOI: 10.1021/cs4002282.

[39] B. G. Mathapa, V. N. Paunov, Cyclodextrin stabilised emulsions and cyclodextrinosomes, Phys. Chem. Chem. Phys., 15 (2013) 17903-17914. DOI: 10.1039/c3cp52116h.

[40] L. Leclercq, A. Mouret, P. Bauduin, V. Nardello-Rataj, Supramolecular colloidosomes based on tri(dodecyltrimethylammonium) phosphotungstate: A bottom-up approach, Langmuir, 30 (2014) 5386-5393. DOI: 10.1021/la500393s.

[41] J. Potier, S. Menuel, E. Monflier, F. Hapiot, Synergetic Effect of randomly methylated β-cyclodextrin and a supramolecular hydrogel in Rh-catalyzed hydroformylation of higher olefins, ACS Catal., 4 (2014) 2342-2346. DOI: 10.1021/cs5004883.

[42] X. Li, H. Li, Q. Xiao, L. Wang, M. Wang, X. Lu, P. York, S. Shi, J. Zhang, Two-way effects of surfactants on Pickering emulsions stabilized by the self-assembled microcrystals of α-cyclodextrin and oil, Phys. Chem. Chem. Phys., 16 (2014) 14059-14069. DOI: 10.1039/c4cp00807c.

[43] L. Leclercq, A. Mouret, S. Renaudineau, V. Schmitt, A. Proust, V. Nardello-Rataj, Self-assembled polyoxometalates nanoparticles as Pickering emulsion stabilizers, J. Phys. Chem. B, 119 (2015) 6326-6337. DOI : 10.1021/acs.jpcb.5b01805.

[44] R. Diaz-Salmeron, I. Chaab, F. Carn, M. Djabourov, K. Bouchemal, Pickering emulsions with α-cyclodextrin inclusions: Structure and thermal stability, J. Colloid Interface Sci., 482 (2016) 48-57. DOI: 10.1016/j.jcis.2016.07.033.

[45] M. Chevry, T. Vanbésien, S. Menuel, E. Monflier, F. Hapiot, Tetronics/cyclodextrin-based hydrogels as catalyst-containing media for the hydroformylation of higher olefins, Catal. Sci. Technol., 7 (2017) 114-123. DOI: 10.1039/c6cy02070d.

[46] B. Pacaud, L. Leclercq, J.-F. Dechézelles, V. Nardello-Rataj, Hybrid core-shell nanoparticles by "plug and play" self-assembly, Chem. Eur. J., 24 (2018) 17672-17676. DOI: 10.1002/chem.201804155.

[47] L. Leclercq, G. Douyère, V. Nardello-Rataj, Supramolecular chemistry and self-organization: a veritable playground for catalysis, Catalysts, 9 (2019) 163. DOI: 10.3390/catal9020163.

[48] B. Yang, L. Leclercq, V. Schmitt, M. Pera-Titus, V. Nardello-Rataj, Colloidal tectonics for tandem synergistic Pickering interfacial catalysis: oxidative cleavage of cyclohexene oxide into adipic acid, Chem. Sci., 10 (2019) 501-507. DOI: 10.1039/c8sc03345e.

[49] H. Taguchi, H. Tanaka, K. Hashizaki, Y. Saito, M. Fujii, Application of Pickering emulsion with cyclodextrin as an emulsifier to a transdermal drug delivery vehicle, Biol. Pharm. Bull., 42 (2019) 116-122. DOI: 10.1248/bpb.b18-00711.

[50] L. Leclercq, J. Tessier, G. Douyère, V. Nardello-Rataj, A. R. Schmitzer, Phytochemical- and cyclodextrin-based Pickering emulsions: natural potentiators of antibacterial, antifungal, and antibiofilm activity, Langmuir, 36 (2020) 4317-4323. DOI: 10.1021/acs.langmuir.0c00314.

[51] Y. Tian, C. Yuan, B. Cui, L. Lu, M. Zhao, P. Liu, Z. Wu, J. Li, Pickering emulsions stabilized by β-cyclodextrin and cinnamaldehyde essential oil/ β-cyclodextrin composite: A comparison study, Food Chem., 377 (2022) 131995. DOI: 10.1016/j.foodchem.2021.131995.

[52] G. Douyère, L. Leclercq, V. Nardello-Rataj, Cross-linked poly(4-vinylpyridine) particles for pH- and ionic strength-responsive "on–off" Pickering emulsions, Colloids Surf. A: Physicochem. Eng. Asp., 631 (2021) 127705. DOI: 10.1016/j.colsurfa.2021.127705.

[53] L. Leclercq, V. Nardello-Rataj, How to improve the chemical disinfection of contaminated surfaces by viruses, bacteria and fungus?, Eur. J. Pharm. Sci., 155 (2020) 105559. DOI: 10.1016/j.ejps.2020.105559.

[54] Health Canada (Government of Canada), Drug product database online query (Search criteria: status = approved, active ingredient = ammonium, class = disinfectant), https://health-products.canada.ca/dpd-bdpp/ (accessed 21 July 2022).

[55] P. C. DeLeo, C. Huynh, M. Pattanayek, K. Clark Schmid, N. Pechacek, Assessment of ecological hazards and environmental fate of disinfectant quaternary ammonium compounds, Ecotoxicol. Environ. Saf., 206 (2020) 111116. DOI: 10.1016/j.ecoenv.2020.111116.

Figures captions

Figure 1. LPEI with adopted representations of protonated and unprotonated amine groups (left inset) and balance between intra- and inter-chain interactions as a function of pH. The right inset shows the various external and internal H-bonds between unprotonated amine groups themselves or with interstitial or superficial water molecules.

Figure 2. Conductivity (**A**, $\kappa \pm 2\%$), equilibrium pH (**B**, $pH_{eq} \pm 2\%$), ζ-potential and stability index (SI) at 30 min (**C**, $\zeta \pm 10\%$ and SI $\pm 4\%$), and hydrodynamic diameter (**D**, $D_h \pm 7\%$) plotted against the initial pH for LPEI aqueous solutions or dispersions (0.1 wt.% in water).

Figure 3. Temperature *versus* pH_{eq} phase diagram of LPEI aqueous samples. The gelation line depends on cooling conditions (1 °C/min, here). In the concomitant gel-sol area (purple) and on cooling, a whitish milky system is observed due to the presence of pseudo-crystalline structures in suspension (local gelation). The insets show the hydrogels as a function of the LPEI concentration (left), a typical microscopic texture under normal and polarized light, and the corresponding interpretation for the 5 wt.% LPEI hydrogel at 25 °C and $pH_{eq} \approx 8$ (right).

Figure 4. Shear viscosity as a function of shear rate at 25 °C and $pH_{eq} \approx 8$ (flow curves, **A**) and shear viscosity as a function of temperature at 100 s^{-1} (**B**) for LPEI hydrogels at different concentrations. The regions *I*, *II* and *III* are only presented for the 2 wt.% LPEI hydrogel.

Figure 5. Macroscopic and microscopic (under normal and polarized light) views of paraffin-in-water emulsions stabilized by 0.5 wt.% LPEI with interpretation (**A**) and backscattering (ΔBS) versus sample height and time at 25 °C for 0.5 and 2 wt.% LPEI emulsions (**B** and **C**, respectively).

Figure 6. Shear viscosity as a function of shear rate at 25 °C (flow curves, **A**) and shear viscosity as a function of temperature at 100 s^{-1} (**B**) for paraffin-in-water emulsions stabilized by at different LPEI concentrations. The insets show the macroscopic and microscopic observations of 2 wt.% LPEI emulsions at 30 and 70 °C (**a** and **b**, respectively).

Figure 7. Frequency dependence of G' and G'' for paraffin-in-water emulsions using different LPEI concentrations.

Figure 8. Thermo-reversibility of paraffin-in-water emulsions stabilized by LPEI (49/49/2 wt.%, 11,500 rpm, 60 s) with emulsion volume fraction over 10 runs.

Figure 9. Alternating stabilization and phase separation by pH trigger of paraffin-in-water emulsion stabilized by LPEI (49/49/2 wt.%, 11,500 rpm, 60 s) with emulsion volume fraction over 3 runs.

Tables

Table 1. Emulsion fraction and log-normal parameters used to fit the droplet size distribution (median diameter, d_m, skewness factor, ω, and amplitude, A) versus time for O/W emulsions at 25 °C.[a]

Oil	Emulsion fraction (v/v)		Droplet size distribution parameters at 24h[b]		
	0h	24h	d_m (µm)	ω	A
Heptane	100	100	38	0.41	428.4
Toluene	100	78	10	0.76	243.6
Isopropyl myristate	100	81	7	0.26	44.7
Liquid paraffin	100	79	1	0.40	74.5
Corn	100	77	1	0.56	35.9
Sunflower	100	91	1	0.53	55.3
Olive	100	54	1	0.50	26.4
Castor	100	87	1	0.54	45.8

[a] Conditions: .5 wt.%, LPEI, 49.75 wt.% water and 49.75 wt.% oil, 11,500 rpm, 60s, 25 °C. [b] Obtained with log-normal function with OriginPro 8®, USA (see Eq. 1).